# Three-dimensional model of the muscle structure and the surface EMG

M. A. Schnetzer[1,2], D. G. Rüegg[1], R. Baltensperger[2] and J. P. Gabriel[2]

[1] Department of Medicine, Division of Physiology, University of Fribourg, Switzerland
[2] Department of Mathematics, University of Fribourg, Switzerland

**Abstract.** The aim of this paper is to describe a spatial model of a muscle including all its motor units (MU) and a simulation of its surface EMG. Elliptic cylinders with a constant ratio between the long and short axis represent the muscle and the MU territories. The distribution of the MU territories is given by an exponential distribution, the small ones being more frequent than the large ones. The fiber densities of the small MUs are smaller than the density of large MUs (linear relation between MU size and density). A problem was the positioning of the MU territories within the muscle cross sectional area with the goal that the sum of all MU densities (global fiber density) is as uniform as possible across the whole muscle cross sectional area. An algorithm that minimizes the variability of the global fiber density each time a new MU is positioned provided the best results. The spatial muscle model obtained in this way was the basis for a simulation of the surface EMG. It is assumed that each muscle fiber generates an action potential (AP) at the motor endplate in the middle of the fiber and that it propagates the AP at constant velocity to both ends. APs were represented by a tripole and the sum of the potentials evoked by the tripoles generates a fiber AP at the recording site. All the fibers within the MU territory generate the MU AP and finally the sum of all active MUs together gives rise to the surface EMG. Simulations with the FDI have shown EMG patterns as found in alive muscles. The proposed model turns out to be adequate to simulate the motoneuron pool muscle complex and provides a powerful tool to investigate mechanisms in muscle activation and motor control.

## 1 Introduction

A skeletal muscle is composed of muscle fibers grouped in motor units (MUs). The number $N$ of MUs in mammalian muscles ranges from ten to several thousands and each one consists of a motoneuron (MN) together with the muscle fibers under its control. The aim of this study was to develop a model of the MU pool, its geometry and the surface EMG evoked by its active MUs.

## 2 The model

### 2.1 Spatial model of motor units

The fiber diameters within a human muscle are assumed to be constant [1],[2]. As in a real muscle, the fibers of a model MU are not scattered throughout the

whole muscle cross sectional area (MCSA) but limited to the MU territory (MUT). A reasonable model for MUTs are ellipses [3] with constant fiber density [4]. The ratio $\beta$ between the major and minor axis and the orientation of the axes are the same for all MUTs. Each MU is characterized by its tetanic contraction force $\tau_i$, $1 \leq i \leq N$. The (continuous) distribution of the MU population as a function of the MU tetanic contraction force is assumed to be exponential [5]. Assuming the same force $\tau$ of all muscle fibers, the contraction force of the MU $i$ is given by:

$$\tau_i = MUT_i \, d_i \, \tau, \tag{1}$$

where $d_i$ is the density of the fibers of the MU $i$. Since $MUT_i = \pi r_i^2/\beta$, the major semi axis of $MUT_i$ is

$$r_i = \sqrt{\frac{\beta \, \tau_i}{\pi \, \tau \, d_i}}. \tag{2}$$

The fiber density is higher in large than in small MUs [6] and it seems reasonable to assume a linear relationship between the MU force and the density:

$$d_i = f + g \, \tau_i, \tag{3}$$

where $f$ and $g$ are constants to be determined. If the fiber density of the smallest MU is $m$ times smaller than the density of the largest MU, we get a system of 3 equations for the unknown variables $f$, $g$, $d_1$ and $d_N$ :

$$\begin{cases} d_1 = f + g \, \tau_1, \\ d_N = f + g \, \tau_N, \\ d_N = m \, d_1. \end{cases}$$

Using $d_1$ as a free parameter, $f$ and $g$ can be determined and put in (3):

$$d_i = \frac{d_1}{\tau_N - \tau_1}(\tau_N - m \, \tau_1 + (m-1) \, \tau_i). \tag{4}$$

Since the total area of the MUTs is $p$ times larger than the MCSA [7], they have to overlap and according to (1):

$$p \, \mathrm{MCSA} = \frac{1}{\tau} \sum_{i=1}^{N} \frac{\tau_i}{d_i}. \tag{5}$$

Replacing $d_i$ in (5) with (4) and solving for $d_1$, we get

$$d_1 = \frac{\tau_N - \tau_1}{p \, \tau \, \mathrm{MCSA}} \sum_{i=1}^{N} \frac{\tau_i}{\tau_N - m \, \tau_1 + (m-1) \, \tau_i}.$$

$d_i$ and $r_i$ can be determined with (4) and (2).

### 2.2 Spatial model of the muscle

The muscle is represented by an elliptic cylinder as the MUs. Its axes are parallel to the MU axes. A major problem was to position the MUs within the MCSA such that the sum of the densities of the overlapping MUs (global density) remains as uniform as possible throughout the whole MCSA. Clearly the ideal solution, i.e. a constant global density cannot be achieved with MUs with a constant fiber density and elliptic MUT. We therefore developed algorithms to place the MUs. In order to attribute a center to a MUT in the MCSA, the MCSA is divided into squares of equal sizes. In this section, the word "point" will refer indifferently to the point in the center of a square and to the square itself. The global density $\delta$ at point $j$ of the muscle is then the sum of the MUT densities at point $A(j)$:

$$\delta(j) = \sum_{i \in A(j)} d_i, \qquad A(j) = \{i; j \in MUT_i\}. \tag{6}$$

Three algorithms were used to place the MUTs. In all of them, the MUTs are positioned according to decreasing size. In the first algorithm, MU centers are positioned randomly within the MCSA. In the second algorithm, all points within the MCSA for which the momentary global density is minimal are determined. One of these points is chosen randomly as MUT center. In the third algorithm, the MUT to be placed is positioned at each point within the MCSA. For each configuration, the variance of the global density is defined by

$$Var(\delta) = \frac{1}{n}\sum_{i=1}^{n}(\delta(j) - \overline{\delta})^2, \quad \text{with} \quad \overline{\delta} = \frac{1}{n}\sum_{j=1}^{n}\delta(j),$$

where $n$ is the total number of points inside the MCSA and $\delta(j)$ is given in (6). The set of points with minimal variance is determined. As in the second algorithm, a randomly chosen point within the set is taken as MUT center.

We positioned 267 MUs of the first dorsal interosseus (FDI) muscle [5] within its circular MCSA. The quality of the global fiber density across the MCSA was tested against uniformity with a $\chi^2$–test (subdivision in 25 cells (resp. 7860)). The third algorithm proved to be much superior to the others ($\chi_1^2 = 2.1 \cdot 10^4$ (resp. $4.2 \cdot 10^4$), $\chi_2^2 = 1.4 \cdot 10^3$ (resp. $1.1 \cdot 10^4$), $\chi_3^2 = 25$ (resp. $2.8 \cdot 10^3$)). The third algorithm was therefore used for modeling the surface EMG.

### 2.3 Model of the surface EMG

In our model, each muscle fiber has a motor endplate in its middle. Action potentials (AP) generated at the postsynaptic membrane are propagated with constant velocity in both directions along the fiber. APs are simulated with a tripole consisting of a current source, followed by a sink and by another source.

A current source $I$ in an unlimited uniform conductor induces a potential $\Phi$ at a distance $D$ given by

$$\Phi = \frac{I}{4\pi c D},$$

where $c$ is the conductivity of the medium.

The conductivity within a muscle is about 5 times larger along than perpendicular to the fiber [8]. Correcting for the anisotropy [9], we get

$$\Phi = \frac{I}{4\pi c_r \sqrt{\frac{r^2 c_z}{c_r} + z^2}},$$

where $r$ and $z$ are the radial resp. longitudinal distance between electrode and motor endplate, $c_r$ the radial and $c_z$ the longitudinal conductivity. Since APs propagate from the endplate in both directions, a fiber AP is determined by 4 weighted current sources ($w_1 I_0$, $w_3 I_0$, $w_4 I_0$ and $w_6 I_0$) and 2 weighted current sinks ($w_2 I_0$ and $w_5 I_0$). The fiber action potential (FAP) is thus given by:

$$\mathrm{FAP}(r,t) = \frac{I_0}{4\pi c_r} \sum_{k=1}^{6} \frac{w_k}{D_k(r,t)},$$

where

$$D_k(r,t) = \sqrt{\frac{r^2 c_z}{c_r} + z_k^2},$$

$I_0$ is a current source of intensity 1 and $z_k$ is the longitudinal distance between electrode and point $k$ of the tripole. The weighting factors $w_k$ are [9]:

$$\begin{aligned} w_1 &= w_4 = 2/3, \\ w_2 &= w_5 = -1, \\ w_3 &= w_6 = 1/3. \end{aligned}$$

At the end of the fiber, the currents decrease linearly and ultimately vanish.

A motor unit action potential (MUAP) is the sum of the potentials evoked by all MU fibers. It is approximated by subdividing the MUT in equidistant grid points. For each fiber passing through such a point, the fiber AP is computed and the potentials generated by all points within $MUT_i$ are added:

$$\mathrm{MUAP}_i(t) = \frac{\tau_i}{\tau C} \sum_{MUT_i} \mathrm{FAP}(r,t).$$

The ratio $\tau_i/\tau$ is the number of fibers and $C$ the number of grid points in $MUT_i$. Adding the MUAPs of the active MUs, we obtain the surface EMG at time $t$ :

$$\mathrm{EMG}(t) = \sum_i \sum_j \mathrm{MUAP}_i(t - t_{ij}),$$

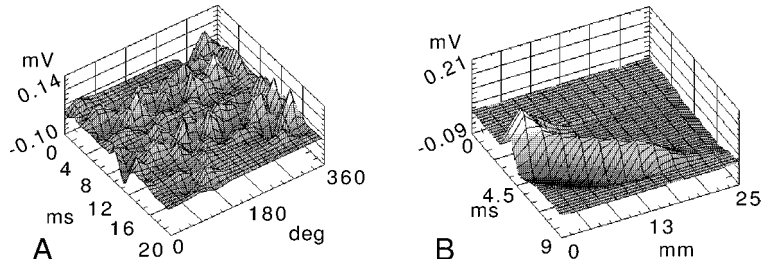


**Fig. 1. A**: Each EMG corresponds to the difference between two neighboring electrodes. $X$-axis: angular position (degrees), $y$-axis: time (ms), $z$-axis: EMG (mV). Several MUs are active. Each MU generates a specific hill within the surface. **B**: Each EMG corresponds to the difference between two neighboring electrodes. $X$-axis: longitudinal position of the center of the two electrodes of an EMG starting at the motor endplates (mm); $y$-axis: time (ms); $z$-axis: EMG (mV). Only one MU is active.

where $t_{ij}$ is the time of occurrence of the $j$-th AP of the MU $i$. The MUs are recruited according to the size principle and frequency modulation [10]. In order to illustrate the performance of the EMG simulation, the FDI was modelled. In the first simulation, 20 electrodes were positioned around the muscle in the plane located 10 mm above the motor endplates. The distance between the surface of the muscle and the electrodes was 2 mm (corresponding to a skin thickness of 2 mm), and the radial angle between consecutive electrodes was 18° (corresponding to 3.86 mm). The muscle was activated at a constant level (activation factor at 1.7, [11]). In Fig. 1A, the 20 EMGs are shown for 20 ms. Most MUAPs have a "triphasic" shape induced by the 3 current sources and sinks. Their duration corresponds to the time of generation at the motor endplate till their disappearance at both muscle ends. In the second simulation, 14 surface electrodes (also 2 mm from the muscle surface) were placed longitudinally along the muscle, starting at the level of the motor endplate. The inter-electrode distance was 2 mm and the last electrode extends 6 mm over the muscle end. Only one MUAP was computed for 9 ms (Fig. 1B). Mainly a positive peak of the MUAP is visible, whereas negative peaks are partly hidden. The two tripoles generated at the motor endplate interact and generate a relatively small MUAP at the first electrode pair and the largest at the second pair. One can observe a linear decrease of the EMG at about 18 mm.

## 3 Conclusion

The basic approach for the computation of the surface EMGs has been developed since a long time [8]. However, the simulation of the 3-dimensional

structure of a muscle, the simulation of its activity, including the recruitment order and the MU rate modulation, and the simulation of the surface EMG were never achieved simultaneously. The major problems about the structure of a muscle was to find all the data required for a realistic reconstruction and to position the MUTs within the MCSA. The simulations have shown that the features of multiple surface EMGs, as found with recordings from human subjects, can be reproduced with the model. The generality of the simulation of the motoneuron-pool-muscle system enables to simulate activation patterns of a variety of human muscles as they occur during normal motor behavior. It will be of special interest to investigate monosynaptic reflexes in the soleus muscle, which is very special in the sense that it has a pennation angle of 30° and very short fibers compared to its length. A further field of interest is to develop algorithms to separate the activity of single MUs from multiple surface recordings.

## References


1. J. Polgar, M. A. Johnson, D. Weightman, and D. Appleton, Data on fibre size in thirty-six human muscles. An autopsy study, *J. Neurol. Sci.*, vol. 19, pp. 307-318, 1973.
2. S. Bodine-Fowler, A. Garfinkel, R.R. Roy, and V.R. Edgerton, Spatial distribution of muscle fibers within the territory of a motor unit, *Muscle Nerve*, vol. 13(12), pp. 1133-45, December 1990.
3. E. Eldred, A. Garfinkel, E. S. Hsu, M. Ounjian, R. R. Roy, and V. R. Edgerton, The physiological cross-sectional area of motor units in the cat tibialis anterior, *Anat. Rec.*, vol. 235(3), pp. 381-9, March 1993.
4. R. E. Burke, and P. Tsairis, Anatomy and innervation ratios in motor units of cat gastrocnemius *J. Physiol.*, vol. 234, pp. 749-765, 1973.
5. R. Nussbaumer, Computer simulation of the motoneuron pool-muscle complex, Doctoral Thesis, Fribourg, 2001.
6. S. C. Bodine, R. R. Roy, E. Eldred, and V. R. Edgerton, Maximal Force as a Function of Anatomical Features of Motor Units in the cat tibialis anterior, *J. Neurophysiol*, vol. 57, pp. 1730-1745, June 1987.
7. L. A. Geddes, and L. E. Baker, The relationship between input impedance and electrode area in recording the Ecg, *Med. Biol. Eng.* vol. 4(5), pp. 439-50, September 1966.
8. S. Andreasson, and A. Rosenfalck, Relationship of intracellular and extracellular action potentials of skeletal muscle fibers, *CRC Crit. Rev. Bioeng.*, vol 6(4), pp. 267-306, November 1981.
9. H. Reucher, J. Silny, and G. Rau, Spatial filtering of noninvasive multielectrode EMG: Part II–Filter performance in theory and modelling, *IEEE Trans. Biomed. Eng.*, vol. 34(2), pp.106-13, February 1967.
10. J. E. Desmedt, Size principle of motoneuron recruitment and the calibration of muscle force and speed in man, in *Motor Control Mechanismus in Health and Disease*, J.E: Desmedt, New York: Raven Press, 1983, pp. 227-251.
11. R. M. Nussbaumer, D.G. Ruegg, L.M. Studer, and J.-P. Gabriel, Computer simulation of the motoneuron pool–muscle complex. I. Input system and motoneuron pool, *Biol. Cybern.*, vol. 86, pp. 317-333, 2002.